

Low Bandgap InAs-Based Thermophotovoltaic Cells for Heat-Electricity Conversion

A. KRIER ^{1,2} M. YIN,¹ A.R.J. MARSHALL,¹ and S.E. KRIER¹

1.—Physics Department, Lancaster University, Lancaster LA1 4YB, UK. 2.—e-mail: a.krier@lancaster.ac.uk

The practical realization of thermophotovoltaic (TPV) cells, which can directly convert heat into electric power, is of considerable technological interest. However, most existing TPV cells require heat sources at temperatures of $\sim 1800^{\circ}\text{C}$. Here we report a low bandgap mid-infrared cell based on InAs and demonstrate TPV operation with heat sources at temperatures in the range $500\text{--}950^{\circ}\text{C}$. The maximum open circuit voltage (V_{oc}) and short circuit current density (J_{sc}) were measured as 0.06 V and 0.89 A cm^{-2} for a blackbody temperature of 950°C and an incident power density of 720 mW cm^{-2} without antireflection coating or electrode optimisation. TPV operation was obtained with heat sources at temperatures as low as 500°C , which represents progress towards energy scavenging and waste heat recovery applications.

Key words: thermophotovoltaic, low bandgap, indium arsenide, waste heat recovery

INTRODUCTION

An efficient, practical, and cost-effective means for directly converting heat into electricity has been the object of much research and development for many years and is a very appealing concept. In principle, thermophotovoltaic (TPV) cells could form the critical component of various systems for generating electricity from different types of heat sources including combustion processes, concentrated sunlight, waste process heat, and radio isotopes. This opens up a wide variety of possibilities for technology uptake and so TPV systems can be envisaged for use in applications ranging from small power supplies to replace batteries, to large scale co-generation of electricity.¹ Further opportunities exist in diverse fields including automotive, power generation, and low-pollution systems for industrial furnaces. In addition to military power applications, there are many commercial, social, and recreational applications, which require a quiet and emission-free compact electrical generator. TPV systems would find uses in remote, backup, and marine power generation as a more reliable and quieter replacement for

diesel generators, especially in locations not suitable for photovoltaic solar arrays or batteries. There is interest in both miniaturizing TPV systems for powering small electronics systems, and scaling-up TPV for large-scale applications such as power plants, submarines, and buildings; as well as for energy recovery from waste heat in the glass, steel, and paper making industries.

TPV cells are solid-state $p\text{--}n$ junction semiconductor devices that directly convert heat into electricity. They absorb the infrared radiation emitted from a hot source and produce electric power by way of the photovoltaic effect. The optimum TPV cell bandgap depends on the radiation spectrum, i.e., the emitter blackbody temperature, and its possible modification by spectral control using a selective emitter, and also on the details of device and system features incorporating photon recycling effects. The main differences between TPV and conventional solar cells are the lower temperature sources found in a TPV system and the much closer proximity of the cell and the extended source. Excellent progress has been made in TPV development² covering a wide range of activities including fundamental and applied research into high-temperature nanophotonics³ and metamaterials⁴ to engineer the selective emitter as well as development of heteroepitaxial

(Received August 14, 2015; accepted January 28, 2016; published online February 18, 2016)

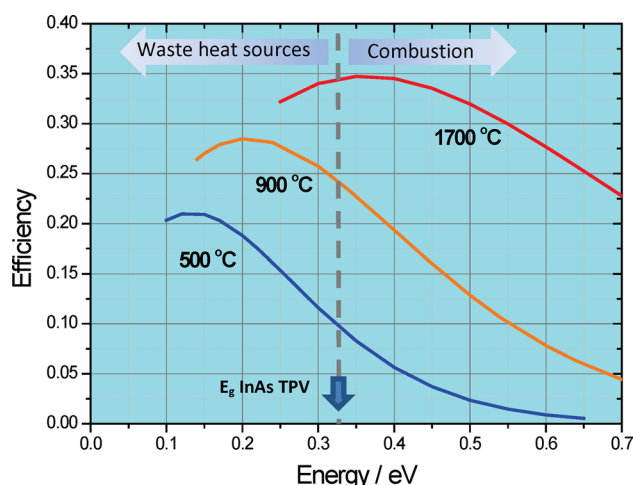


Fig. 1. Maximum efficiency for a TPV cell. The dependence of TPV efficiency on bandgap for blackbody sources at different temperatures derived from the Shockley Queisser detailed balance model.³ Figure adapted from Cody.² In combustion, normally source temperatures are $>1800^{\circ}\text{C}$, whereas for waste heat recovery sources are much cooler, typically $500\text{--}1000^{\circ}\text{C}$, which requires TPVs with lower bandgaps.

III–V semiconductor devices^{5,11} and micron-gap or near-field heat transfer methods,⁶ as well as complete system demonstrations.⁷ In this work we are concerned only with the development of the TPV cell. As shown in Fig. 1, theoretical modelling⁸ following the thermodynamic detailed balance model of Shockley and Queisser,⁹ shows that in the ideal case where radiative recombination is dominant, for temperatures below 1700°C , the maximum cell conversion efficiency is obtained using bandgaps below 0.5 eV . However, previous work has concentrated on TPV devices matched to high temperature combustion sources using semiconductors with larger bandgaps such as silicon with $E_g = 1.1\text{ eV}$, InGaAs¹⁰ on InP—typically $E_g = 0.5\text{--}0.73\text{ eV}$, but which is limited by lattice mismatch to the higher bandgap ranges - or InGaAsSb on GaSb, which is constrained to $E_g = 0.5\text{ eV}$ by a miscibility gap. More recently, GaSb $p\text{--}i\text{--}n$ photodiodes have been grown on GaAs (100) substrates for use as TPV cells using the interfacial misfit array method to reduce substrate costs.^{11,12}

There have been a few previous works, which described the successful epitaxial growth, development, and characterization of lower bandgap InAs-based materials and diodes for TPV applications.^{13–17} However, to date there are no reports of TPV characteristics in response to blackbody radiation at temperatures below 1000°C as required for waste heat recovery applications. More recently, metallic photonic crystals have been developed as thermal emitters¹⁸ for spectral shaping in TPV systems, and theoretical work has proposed Graphene-assisted Si-InSb for low temperature TPV applications.¹⁹ Meanwhile, there are currently active investigations into more complex architectures using quantum cascade-based or multiple-

junction TPVs, which show great promise, but there are still no commercial TPV cells available for the thermal source temperatures below 1000°C .^{20–22} In this work we have demonstrated a TPV response from a blackbody source at temperatures as low as 500°C using a cell with an InAs active region with a bandgap of 0.32 eV at 300 K .

EXPERIMENTAL PROCEDURES

The cell design implemented here is shown in Fig. 2a and was fabricated using liquid phase epitaxial (LPE) growth on an n -type InAs substrate. The structure comprises a lattice-matched quaternary alloy layer of p -type InAsSbP as a window layer with wider bandgap of $\sim 0.5\text{ eV}$ to allow light in and reduce surface recombination of photo-generated carriers. The InAs active region is $4\text{ }\mu\text{m}$ in thickness to provide effective absorption. To reduce the residual carrier concentration in the InAs active region, we employed a Gd gettering technique to remove impurities from the active region during growth.²³ Epitaxial layers of unintentionally doped InAs and p -type Zn-doped $\sim 1 \times 10^{18}\text{ cm}^{-3}$, quaternary InAsSbP were grown nominally lattice-matched onto n -type, $2 \times 10^{18}\text{ cm}^{-3}$ InAs (100) substrates by conventional LPE using a horizontal sliding boat technique. Growth was implemented from In-rich melts at temperatures within the interval of $570\text{--}580^{\circ}\text{C}$ based on our previous work,¹⁰ using supercooling, $\Delta T \sim 3^{\circ}\text{C}$. The alloy composition of the quaternary alloy as determined by energy dispersive x-ray analysis was found to be InAs_{0.61}Sb_{0.13}P_{0.26}. The resulting layers were also characterised using photoluminescence (PL) spectroscopy in the temperature range $4\text{--}300\text{ K}$. PL was excited using an Ar⁺ ion laser (514 nm), which produced an excitation density of 20 W cm^{-2} at the sample surface. The InAs bandgap was found to be in agreement with the results from the spectral response measurements in Fig. 3. Hall Effect measurements using the Van der Pauw method were used to obtain the residual carrier concentration, which was $\sim 1 \times 10^{16}\text{ cm}^{-3}$.

The TPV cells were fabricated by standard ultra-violet photolithography and wet chemical etching techniques, with a mesa etch depth of $\sim 6\text{ }\mu\text{m}$. Metal contacts were realized using thermal evaporation and consisted of Ti-Au or Ni-Au alloys. The mesa area was designed as $1\text{ mm} \times 1\text{ mm}$, with a nine finger electrode pattern. No anti-reflection coating or passivation of the cells was used. The spectral response was measured with a calibrated blackbody at a temperature of 1200 K using a grating monochromator, blazed at $3.5\text{ }\mu\text{m}$, and lock-in amplifier with a chopper frequency of 180 Hz . The results were corrected and normalised using a pyroelectric detector with a flat response. For the efficiency measurements, a variable temperature blackbody of $500\text{--}1200^{\circ}\text{C}$ with an aperture of 25 mm was used as the thermal source. The optical

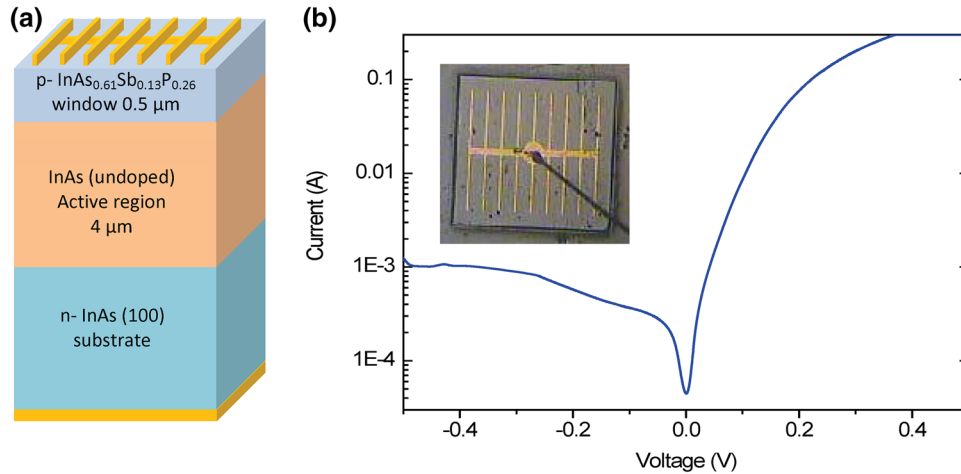


Fig. 2. (a) The InAs TPV cell design showing the layer structure of the low bandgap cell, (b) the current voltage characteristic of the TPV cell in the dark; the inset shows a microscope image of the completed processed cell, with mesa dimensions $1\text{ mm} \times 1\text{ mm}$ and contact electrodes $50\text{ }\mu\text{m}$ wide.

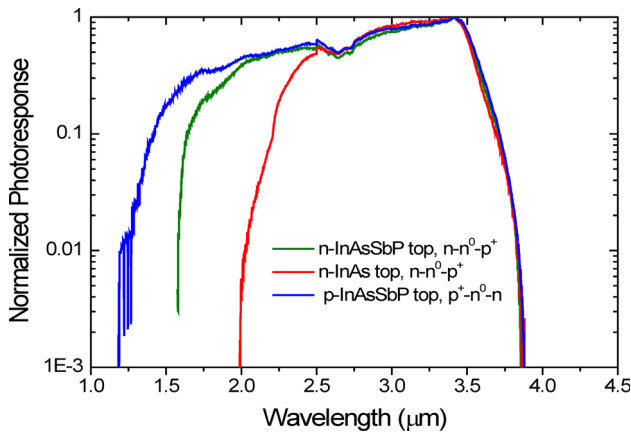


Fig. 3. The spectral response of InAs TPV cells having different windows. The response extends to shorter wavelengths for TPV cells with quaternary window layers, but the long wavelength cut-off remains the same. Blue: $p\text{-InAsSbP}$ window; green: $n\text{-InAsSbP}$ window; red $n\text{-InAs}$ window (Color figure online).

(thermal) power incident on the surface of the TPV cell was measured using a 10 mm diameter large-area thermopile; a Melles Griot 13 PEM 001/J power meter, constructed from a high-density graphite disc having a uniformity of 81% over the central 8 mm and a dynamic range from $2\text{ }\mu\text{W}$ to 2 W . In all cases the TPV cell was positioned normal to the incident radiation and a correction was made to account for the field of view of the thermopile. For completeness, the efficiency was also measured with the TPV cell at room temperature using a calibrated Landcal P550P blackbody source at 500°C with a 65 mm diameter aperture.

RESULTS AND DISCUSSION

Figure 2(b) shows the dark current–voltage (I – V) characteristic from one of the TPV cells, from which the ideality factor was obtained as 1.4, with a shunt

resistance of $217\text{ }\Omega$ and a series resistance of $0.75\text{ }\Omega$ at 300 K . A comparison of the photoresponse of $p\text{-i-n}$ and $n\text{-i-p}$ cell structures having different window layers is shown in Fig. 3, where the atmospheric absorption near $2.7\text{ }\mu\text{m}$ arises from water vapour in the optical path. In each case the long wavelength cut-off is obtained as $3.86\text{ }\mu\text{m}$ (0.32 eV) associated with absorption in the InAs active region, which is a little smaller than the intrinsic 300 K InAs band gap due to the Urbach tail states. We observed that cells with a p -type InAsSbP window layer exhibited a broader photoresponse extending down to a minimum wavelength of $1.25\text{ }\mu\text{m}$. High energy photons are collected by the window layer, although the corresponding photogenerated carriers are subject to near surface recombination. The extended short wavelength photoresponse for the p -type InAsSbP window material is due to the proximity of the p – n junction to the front of the device. In the case of the p -type InAsSbP window, the minority carriers generated in the window only need to diffuse $0.5\text{ }\mu\text{m}$ before they are collected by the p – n junction and become majority carriers. Electrons generated in the p -type InAsSbP window layer and emitted into the active region are able to transit across the InAs active region without recombining, due to the longer minority carrier diffusion length. For the other samples, the minority carriers (holes) need to diffuse $4.5\text{ }\mu\text{m}$ in order to be collected.

The output from the TPV cell at room temperature (20°C) is shown in Fig. 4a for blackbody source temperatures in the range 500°C – 950°C , where the total incident power increases as the source temperature increases. Due to the low bandgap of the InAs, 0.32 eV as determined from the spectral response in Fig. 3, the cell generates power at low source temperatures within the range suitable for waste heat recovery applications. The maximum open circuit voltage (V_{oc}) and short circuit current density (J_{sc}) were measured as 0.06 V and

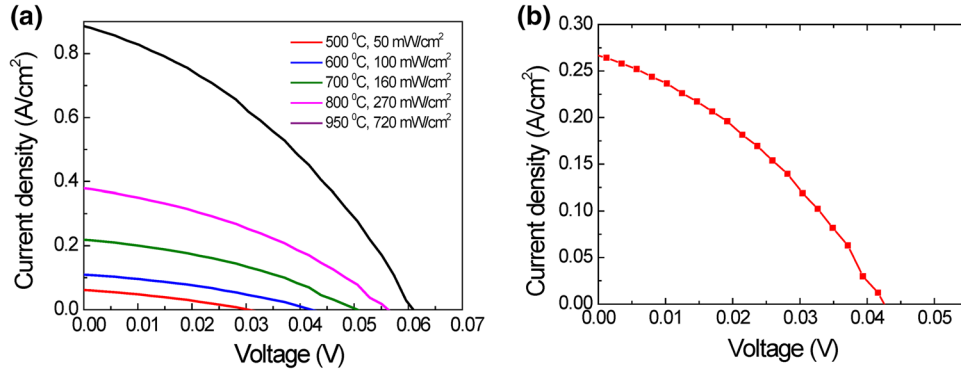


Fig. 4. (a) The TPV response, current density–voltage (J versus V) of the cell, obtained using a blackbody at different temperatures in the range 500–950°C. The corresponding incident power density at each temperature is given in the legend; (b) The current density versus voltage characteristic of the InAs-based TPV cell at room temperature (20°C) exposed to a blackbody source at 500°C. The power incident on the cell was 800 mW cm⁻² (Color figure online).

0.89 A cm⁻² for a blackbody temperature of 950°C and an incident power density of 720 mW cm⁻². The fill factor was obtained as 37% with a corresponding power output of 20 mW cm⁻² and conversion efficiency of ~3%, after correcting for current collection outside the defined mesa area and obscuration by the metal electrode, without anti-reflection coating or contact electrode optimization. Figure 4b shows the TPV output from the cell (at 20°C) in response to a blackbody source at 500°C using an incident power density of 800 mW cm⁻². The measured open circuit voltage, (V_{oc}) was ~0.04 V and short circuit current density, (J_{sc}) was 0.27 A cm⁻² with a corresponding fill factor of 36%. The power output was 4 mW cm⁻² with conversion efficiency of 0.5%, which is consistent with the detuning of the blackbody output with respect to the InAs TPV cell bandgap of 0.32 eV at room temperature.

As expected the value of $V_{oc} = 0.06$ V is much smaller than the value of $V_{oc} = 0.24$ V obtained from thermodynamic considerations.² The open circuit voltage V_{oc} and short circuit current density J_{sc} for a photovoltaic cell are given by;

$$V_{oc} \approx \left(\frac{kT}{q} \right) \ln \left(1 + \frac{J_{sc}}{J_0} \right) \quad (1)$$

$$J_0 \approx q \left(\frac{D_n n_i^2}{L_n N_A} + \frac{D_p n_i^2}{L_p N_D} \right) \quad (2)$$

where, n_i is the intrinsic carrier concentration, q is the electron charge, D_n (D_p) is the electron (hole) diffusion coefficient, L_n (L_p) is the effective minority carrier diffusion length, N_D (N_A) is the donor (acceptor) doping concentration, and J_0 is the reverse saturation current density. Using representative values from the literature²⁴ for the terms in Eq. 2 we obtained a value of $J_0 = 0.13$ A cm⁻², which is in agreement with the measured value of 0.10 A cm⁻², and which is also consistent with the measured value of V_{oc} . It is well known that InAs alloys are subject to surface accumulation, but in

this case we consider that our prototype cells are dominated by bulk leakage, which is further confirmed by comparing devices of different perimeter to area ratios. With reference to Eq. 2, this is primarily a result of the high intrinsic carrier concentration in InAs (~10¹⁵ cm⁻³) and the minority carrier lifetime (diffusion length).¹⁰

CONCLUSIONS

In summary, we have demonstrated a TPV response from a blackbody source at temperatures as low as 500°C using a prototype low bandgap InAs-based TPV cell. The maximum open circuit voltage (V_{oc}) and short circuit current density (J_{sc}) were measured as 0.06 V and 0.89 A cm⁻² for a blackbody temperature of 950°C and an incident power density of 720 mW cm⁻². The fill factor was obtained as 37% with a corresponding efficiency of 3% without antireflection coating or electrode optimisation. TPV output was still obtained from a 500°C blackbody where the cell efficiency reduced to 0.5%. These cells are currently only suitable for applications with low power requirements such as energy scavenging devices, battery chargers, low power electronics, and sensors.²⁵ Although V_{oc} can be increased by increasing the incident power density, our results show that to achieve higher efficiencies necessary for practical implementation, more complex structures based on either monolithic interconnected modules (MIMs),²⁶ or interband cascade architectures are needed to significantly increase the open circuit voltage. Further work is also required to implement the low bandgap InAs TPV elements in the form of a monolithic array. However, our results show that InAs-based cells can provide a possible route towards the development of TPVs for energy conversion from waste heat sources at temperatures as low as 500°C.

ACKNOWLEDGEMENTS

Financial support for this work was provided by the UK Technology Strategy Board in collaboration

with CST Global, IQE Ltd., Tata Steel, and Pilkington Ltd. under Grant No: TP11/LCE/6/TAE096F and EPSRC Grant EP/M013707/1.

OPEN ACCESS

This article is distributed under the terms of the Creative Commons Attribution 4.0 International License (<http://creativecommons.org/licenses/by/4.0/>), which permits unrestricted use, distribution, and reproduction in any medium, provided you give appropriate credit to the original author(s) and the source, provide a link to the Creative Commons license, and indicate if changes were made.

REFERENCES

1. M.G. Mauk and V.M. Andreev, *Semicond. Sci. Technol.* 18, S191–S201 (2003).
2. See EU PVSEC 2016 for example TPV papers from the European PV solar energy conferences available at: <https://www.photovoltaiac-conference.com/93-27th-eu-pvsec/parallelevents/1636-tpv-10conference-2012.html> (2012).
3. N.A. Pfister, D.F. DeMeo, C.M. Shemela, and T.E. Vandervelde, *J. Electron. Mater.* 41, 928 (2012).
4. D. Woolf, J. Hensley, J.G. Cederberg, D.T. Bethke, A.D. Grine, and E.A. Shaner, *Appl. Phys. Lett.* 105, 081110 (2014).
5. S.L. Murray, F.D. Newman, C.S. Murray, D. M. Wilt, M.W. Wanlass, P. Ahrenkiel, R. Messham, and R.R. Siegij, *Semicond. Sci. & Technol.* 18, S202 (2003).
6. R. DiMatteo, P. Greiff, D. Seltzer, D. Meulenberg, E. Brown, E. Carlen, K. Kaiser, S. Finberg, H. Nguyen, J. Azarkevich, P. Baldasaro, J. Beausang, L. Danielson, M. Dashiell, D. DePoy, H. Ehsani, W. Topper, K. Rahner, and R. Siegij, *AIP Conference Proceedings* (2004) vol. 738, p. 42.
7. W.R. Chan, C.M. Waits, J.D. Joannopoulos, and I. Celanovic, *Micro Nanotechnol. Sens. Syst. Appl.* VI 9083, 90831W (2014).
8. G.D. Cody in T.J. Coutts, J.P. Benner, and C.S. Allman (Eds.), *AIP Conference Proceedings* (1998), vol. 450, p. 58.
9. W. Shockley and H.J. Queisser, *J. Appl. Phys.* 32, 510 (1961).
10. R.S. Tuley and R.J. Nicholas, *J. Appl. Phys.* 108, 084516 (2010).
11. D. DeMeo, C. Shemelya, C. Downs, A. Licht, E.S. Magden, T. Rotter, C. Dhital, S. Wilson, G. Balakrishnan, and T.E. Vandervelde, *J. Electron. Mater.* 43, 902 (2014).
12. B.C. Juang, R.B. Laghumayarapu, B.J. Foggo, P.J. Simmonds, A. Lin, B.L. Liang, and D.L. Huffaker, *Appl. Phys. Lett.* 106, 111101 (2015).
13. V.A. Gevorkyana, V.M. Aroutiouniana, K.M. Gambaryana, M.S. Kazaryana, K.J. Touryanb, and M.W. Wanlassb, *Thin Solid Films* 451, 124 (2004).
14. V.A. Gerorkyan, V.M. Aroutiounian, K.M. Gambaryan, I.A. Andreev, L.V. Golubev, and Y.P. Yakovlev, *Tech. Phys. Lett.* 34, 69 (2008).
15. M.G. Mauk, O.V. Sulima, J.A. Cox, and R.L. Mueller, in K. Kurokawa, L.L. Kazmerski, B. McNelis, M. Yamaguchi, C. Wronski, and W.C. Sinke, eds., *Proceedings of 3rd World Conference on Photovoltaic Energy Conversion* (2003) vol. A-C, p. 224.
16. V. Andreev, V. Khvostikov, O. Khvostikova, N. Kaluzhnyi, E. Oliva, V. Rumyantsev, S. Titkov, and M. Shvarts in K. Kurokawa, L.L. Kazmerski, B. McNelis, M. Yamaguchi, C. Wronski, and W.C. Sinke, eds., *Proceedings of 3rd World Conference on Photovoltaic Energy Conversion* (2003) vol. A–C, 15.
17. O.V. Sulima, A.W. Bett, M.G. Mauk, F. Dimroth, P.S. Dutta, and R.L. Mueller in T.J. Coutts, G. Guazzoni, and J. Luther, eds., *Thermophotovoltaic Generation of Electricity, AIP Conference Proceedings* (2003), vol. 653, p. 434.
18. P. Nagpal, S.E. Han, A. Stein, and D.J. Norris, *Nano Lett.* 8, 3238 (2008).
19. M. Lim, S. Jin, S.S. Lee, and B.J. Lee, *Opt. Express* 23, A240 (2015).
20. J. Yin and R. Paiella, *Opt. Express* 18, 121393 (2010).
21. Z.B. Tian, R.T. Hinkey, R.Q. Yang, J.F. Klem, and M.B. Johnson, *38th IEEE Photovoltaic Specialists Conference (PVSC)* (Austin, TX JUN 03-08, 2012), pp. 1560–1565.
22. R.T. Hinkey, Z.-B. Tian, S. Rassel, R.Q. Yang, J.F. Klem, and M.B. Johnson, *IEEE J. Photovolt.* 3, 745 (2013).
23. H. Gao, A. Krier, and V. Sherstnev, *Semicond. Sci. Technol.* 14, 441 (1999).
24. <http://www.ioffe.ru/SVA/NSM/Semicond/InAs/>.
25. M. Gorlatova, A. Wallwater, and G. Zussman, *IEEE Trans. Mob. Comput.* 12, 1853 (2013).
26. D.M. Wilt, N.S. Fatemi, P.P. Jenkins, V.G. Weizer, R.W. Hoffmann, R.K. Jain, C.S. Murray, and D.R. Riley, in T.J. Coutts, C.S. Allman, and J.P. Benner, eds., *Proc. 3rd NREL Thermophotovoltaic Generation of Electricity Conf., AIP Conference Proceedings* (1997), vol. 40, p. 237.